THE ARCHIVE OF MECHANICAL ENGINEERING

Vol. LI 2004 Number 3

Key words: *crack closure, fatigue crack growth, fatigue test*

*MAŁGORZATA SKORUPA**), *ANDRZEJ SKORUPA**), *TOMASZ MACHNIEWICZ**)

DETERMINATION OF CRACK CLOSURE FOR STRUCTURAL STEEL FROM LOCAL COMPLIANCE RECORDS

The usefulness of elastic compliance measurements to estimate crack closure in structural steel and the validity of the assumption of a constant compliance value for the fully open crack is examined. Based on considering different issues related to the experimental technique and compliance data processing, local compliance measurements and the compliance offset method recommended by the ASTM standard are selected to be most suitable for structural steel. The compliance data generated in fatigue tests on 18G2A steel conducted under a variety of loading conditions enabled to choose an optimal strain gauge positioning and appropriate offset criterion values for the original compliance offset method and its modified (normalized) version. The adequacy of the closure measurements is assessed through checking the ability of the resulting effective stress intensity factors to account for the observed effects of the loading conditions on fatigue crack growth rates.

1. Introduction

In 1971, Elber [1] noted experimentally that contact between the fatigue crack surfaces could occur during tensile portions of load cycles. Such a phenomenon associated with load transmission through the contact area is generally referred to as crack closure (CC), which is thought to reduce the crack driving force in fatigue. The concept of CC leads to the assumption, first adopted by Elber, that crack propagation conditions only exist when the crack is fully open. The range of stress intensity effective for causing crack growth (ΔK_{eff}) is then defined by

$$\Delta K_{\text{eff}} = K_{\max} - K_{\text{op}} \tag{1}$$

*) *AGH University of Science and Technology, Al. Mickiewicza 30, 30-059 Kraków, Poland; E-mail: mskorupa@uci.agh.edu.pl*

where K_{max} is the maximum value of the stress intensity factor and K_{op} is the so called crack opening level at which the crack fully opens on loading, Fig.1. The CC concept implies that, for a given material and environmental conditions, the fatigue crack growth rate (da/dN) in a given loading cycle is a unique function of the ΔK_{eff} parameter.

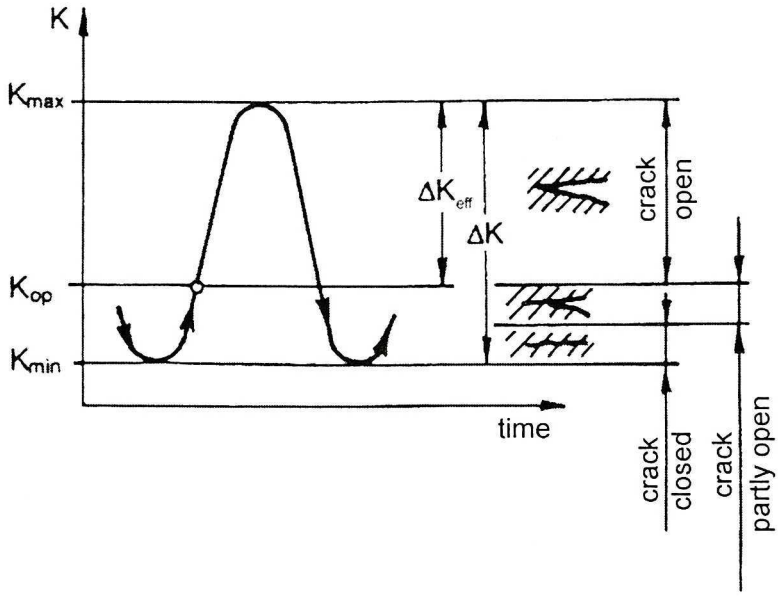

Fig. 1. Parameters related to crack closure

Elber attributed CC to the presence of residual plastic deformations in the fatigue crack wake. Subsequent work has identified other contributory factors to the CC process, including fracture surface roughness and environmental debris. The technical significance of CC stems from the fact that it enables to rationalize many crack growth characteristics, for example the effects of stress ratio (R), thickness (t), and material mechanical properties, the load interaction phenomena which typically occur under variable amplitude (VA) loading, the small crack effect, and the threshold behaviour [2]. In view of that, CC has become one of the most intensively studied phenomena associated with crack growth and is a key aspect of modern crack growth prediction models.

Though a variety of CC measurement methods have been proposed (see reviews in Refs [2], [3]), none of them has been commonly accepted. However, because of limitations and inconveniencies involved in application of various techniques, the mechanical compliance method remains the most often used experimental tool. With the latter method, the crack opening load

(P_{op}) is estimated from the compliance P-ε data, where P is the applied load and ε is the strain or displacement captured throughout the fatigue cycle in an elastic region of the specimen. If CC occurs in a fatigue cycle, the compliance curve is linear only when the crack is fully open at $P>P_{op}$, i.e. above point B in Fig. 2a. At $P<P_{op}$, the curve slope (at the same time an inverse of the specimen compliance $c = \varepsilon/P$) increases with decreasing the load level because a gradual closing of the fatigue crack is associated with a decrease in the effective crack length.

Identifying the P_{op} level from the compliance record, though conceptually straightforward, is a very difficult and complicated task. With the real measurement data, Fig. 2b, the difficulties stem from the nonlinearity often shown not only below P_{op} but also by the whole compliance curve, the compliance data hysteresis, and measurement noise. An extensive review and evaluation of approaches proposed to determine P_{op} from compliance records is provided elsewhere [3], [4].

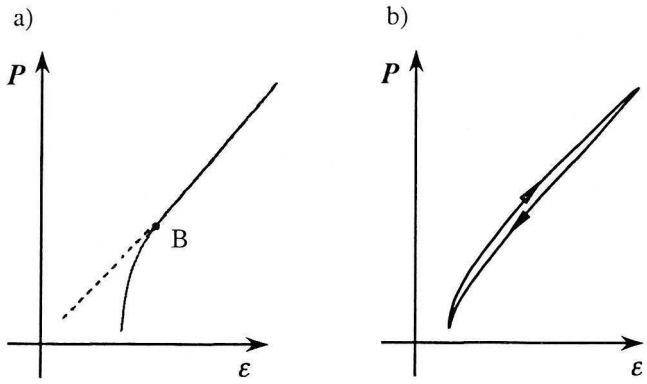

Fig. 2. Ideal (a) and real (b) compliance curve

Typically, however, P_{op} is identified based on the assumption that the specimen compliance remains constant for the fully open crack. Some procedures of this type, among them the widely used method recommended by the ASTM standard [5], consider variations in the slope of the compliance curve. To reduce the impact of measurement noise, the ASTM method models the loading branch of the P-ε curve employing a sequence of partly overlapping linear segments, each addressing a small load interval, as shown in Fig. 3a. For segment i, the compliance offset parameter is defined as

$$CO_i = \frac{c_{op} - c_i}{c_{op}} \cdot 100\% \tag{2}$$

where the c_{op} is the "open crack" compliance determined for a least-squares straight line fitting the unloading branch of the P-ε curve within the uppermost 25% of the cyclic load range and c_i is the compliance of segment i. A preset deviation in CO_i (the so-called compliance offset criterion) from the fully open value, i.e. from $CO_i = 0$, defines the P_{op} level, as seen in Fig. 3b.

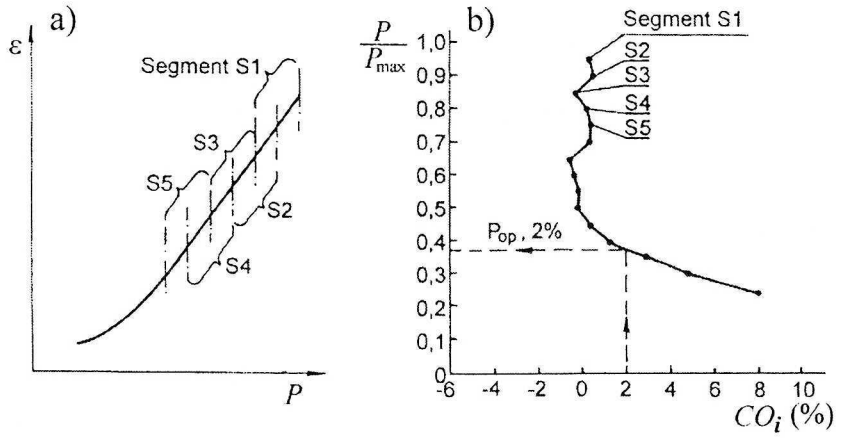

Fig. 3. Determination of P_{op} using the ASTM method [5]

With the normalized ASTM procedure proposed by Song and Kang [6] and referred to as the nASTM method, a CO_i/CO_{max} parameter, where CO_{max} is the maximum value of the compliance offset in a fatigue cycle, is used instead of CO_i. Based on CC measurements in an Al alloy, the latter authors claim that compared to the ASTM procedure the nASTM method enables a better correlation of the R-ratio effect on crack growth.

Alternatively, "global" curve fitting is also used to determine P_{op}. Usually, a second order polynomial is fitted to the lower part of the compliance curve whilst for the upper region a linear curve fit is applied (e.g. [7], [8], [9]). The resulting P_{op} value corresponds to the tangency point or to the intersection point of both curves.

Another approach, first proposed by Kikukawa et al. [10], employs an offset strain parameter defined as

$$\varepsilon_{offset} = k\,(\varepsilon - c_{op} P) \tag{3}$$

where c_{op} is the specimen compliance for the fully open crack, and k is the amplification coefficient. Often the data processing according to Eq. (3) is performed through analogue operations on the ε and P electric signals [10]. For an ideal compliance curve shown in Fig. 2a, $\varepsilon_{offset} = 0$ when the crack is

fully open. Hence, the P_{op} value corresponds to the preset deflection of the P vs. ε_{offset} diagram from the $\varepsilon_{offset} = 0$ vertical line. With real measurement data shown in Fig. 2b, the identification of P_{op} is much less obvious because the P-ε_{offset} plot may be curvilinear and exhibit hysteresis.

P_{op} estimates from any procedure of processing the compliance records depend upon assumptions about selecting the upper portion of the data for the linear fit and on preset criteria for identifying the closure point. It is also evident that the compliance data quality plays a crucial role. It cannot be overlooked that the impact of the data quality is felt more strongly when considering the derivatives of the signal rather than the original record. Hence, P_{op} estimates from the slope analysis methods or from the ε_{offset} method can be more critically affected by the presence of noise than those from the curve fitting procedures.

CC measurements can be performed using either a remote or a local compliance technique. With the first of these, the compliance data are captured employing a single strain gauge positioned far from the crack tip, whilst a series of near tip surface strain gauges mounted at various locations relative to the crack line are used for the local compliance measurements.

The adequacy of a given configuration of the measurement technique and the procedure of estimating P_{op} levels is usually assessed by the ability of the resulting ΔK_{eff} parameter to correlate the observed effects of the R-ratio on da/dN in CA tests, and to account for the post-overload crack growth transients. The scatter in the P_{op} results can also be a measure of the robustness of a given method.

Because of the unquestionable convenience of the remote CC measurements compared to the local technique, systematic comparisons of both methods can be found in the literature. For an Al alloy under CA loading conditions, Xu et al. [9] reported that the curve fitting method provided consistent P_{op} results derived from both techniques. For structural steel, however, the combination of linear and quadratic functions is not suitable to approximate either remote or local compliance data [3]. A small extent of nonlinearity shown by the compliance diagram is uniformly distributed within the whole load range rather than concentrated below the P_{op} level, as with Al alloys. Hence, CC for structural steel is usually estimated using the slope analysis procedures or the ε_{offset} method. An inconsistency of the slope analysis methods between remote and local compliance measurement results on P_{op} under CA loading has been noted for various metals in several works, e.g. [9], [10], [11]. CC estimates obtained by Tokaji et al. [12] for a structural steel via the ε_{offset} method and results for a modified steel derived by Dougherty [11] using a slope analysis procedure demonstrated that unlike the

local compliance measurements, the remote technique was not capable of detecting CC transients following the overload (OL) application.

The literature evidence on the ability of the ΔK_{eff} parameter derived from various compliance techniques and data analysis procedures to correlate fatigue crack growth rates under various loading conditions is conflicting. One can find both results demonstrating a good consolidation of the da/dN vs. ΔK_{eff} data into a single curve over a range of R-ratios (e.g. [13], [14] for structural steel) and results indicating that the R-ratio effects do not wholly disappear in the da/dN vs. ΔK_{eff} plot (e.g. [15], [16] for structural steel). In all four works cited above, the CC levels were estimated employing the ε_{offset} method from either global [13] or local [15], [16] compliance measurements. With Ref. [14], the measurement technique is not reported.

Given the above confusing results, an extensive experimental program has been realized to develop an optimum CC measurement methodology for structural steel. A part of the research reported in the present paper aimed at checking the utility of the conventional approach, i.e. of identifying P_{op} based on the assumption of a constant compliance for the fully open crack. Out of this type procedures applicable to structural steel, the ε_{offset} method is more subjective in identifying the closure point and more sensitive to measurement noise than the slope variation methods. Consequently, the P_{op} results from the ε_{offset} method show more scatter, as demonstrated for an Al alloy by Song and Kang [6]. Though for Al alloys, the ASTM procedure remains a most widely used approach, its adequacy for structural steel remains unknown. In view of that, the ASTM method has been selected for application in the present study in both the original and the normalized (nASTM) version. Though the ASTM standard favours the remote compliance data, the local compliance records will be used here because of their undeniably higher sensitivity noted in the aforementioned studies [9], [11], [12]. The latter aspect is of particular importance for considering the correlation between observed post-OL fatigue crack growth rates and those predicted from the measured CC response.

2. Experimental

2.1. Fatigue crack growth tests

The material used was low carbon structural steel 18G2A (according to PN-EN 10028 standard), for which the mechanical monotonic and cyclic properties (6 mm thick sheet specimens and 8 mm dia specimens respectively) and chemical composition are specified in Table 1. All

experiments were conducted on a servo-controlled, hydraulically actuated closed-loop fatigue machine interfaced to a computer for operating the machine and data acquisition. The fatigue cracks were generated under load control using middle crack tension specimens 100 mm in width and 4, 12 and 18 mm in thickness. The central starter notch 16 mm in length was made by electrical-discharge machining. Depending on the load conditions, the loading frequency ranged between 10 and 30 Hz except when the CC measurements were made, as explained later on. The crack length was monitored with an accuracy of ± 0.01 mm using a traveling microscope with a magnification of $150\times - 300\times$. A survey of the experiments is given in Table 2. It is seen that, apart from the Type CA tests conducted under constant amplitude (CA) loading at a range of R-ratios and at various applied stress levels, and two tests under 2-step loading (Type 2CA), the experiments included also several tests with a single OL applied among smaller amplitude cycles (Type OL and 2OL). The fatigue tests were carried out until complete fracture of the specimens. The observed crack growth rates corresponded to stage II and III crack growth and spanned a range from 10^{-6} to 4×10^{-4} mm/cycle, the lowest da/dN values being measured during the post-OL transient retardation in crack growth.

Table 1.

Mechanical properties and chemical composition of the 18G2A steel

Mechanical properties:							
Monotonic			Cyclic				
Yield stress S_y, MPa	Ultimate strength S_U, MPa	Elongation to failure ε_f, %	Yield stress $S_{y0.005}$, MPa	Strength coefficient K, MPa	Strain-hardening exponent, n		
398	540	25	265	1014.5	0.177		
Chemical composition, %							
C	Mn	Si	P	S	Cu	Cr	Ni
Analysis							
0.14	1.36	0.21	0.02	0.02	0.12	0.11	0.05
Standard PN-EN 10028							
max 0.22	1-1.16	0.2-0.55	max 0.05	max 0.05	max 0.12	max 0.11	max 0.3

Table 2.

Survey of the fatigue tests and closure measurement methods

Test No.	CC measurement method	Specimen thickness t, mm	Stress ratio R	Stress levels, MPa			Test type
				S_{min}	S_{max}	S_{OL}	
0225	II	4	−1	−55	55	–	CA
0205	I		0.05	4.3	84.3	–	
0220	II		0.15	14.1	94.1	–	
0221	II		0.5	80	160	–	
0211	–		0.7	116.8	166.8	–	
0202	I	12	0.05	4.3	84.3	–	
0212	–		0.7	116.8	166.8	–	
0213	I	18	0.05	4.1	79.6	–	
0218	I			4.3	84.3	–	
0222	II	4	0.15	9.1	59.5	–	2CA
0223	II		0.51	52	102		
0210	I	4	0.05	4.3	84.3	164.3	OL
0209	I		0.5	80	160	240	
0208	I	12	0.05	4.3	84.3	164.3	
0214	I	18	0.05	4.1	79.6	155.2	
0224	II	4	0.07	3.6	53.6	102.6	2OL
			0.04	3.6	83.6	143.6	

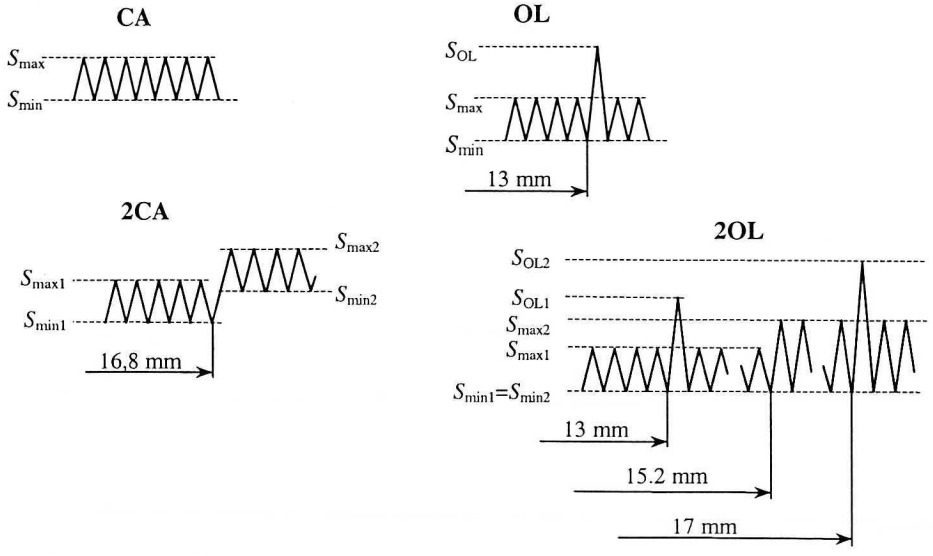

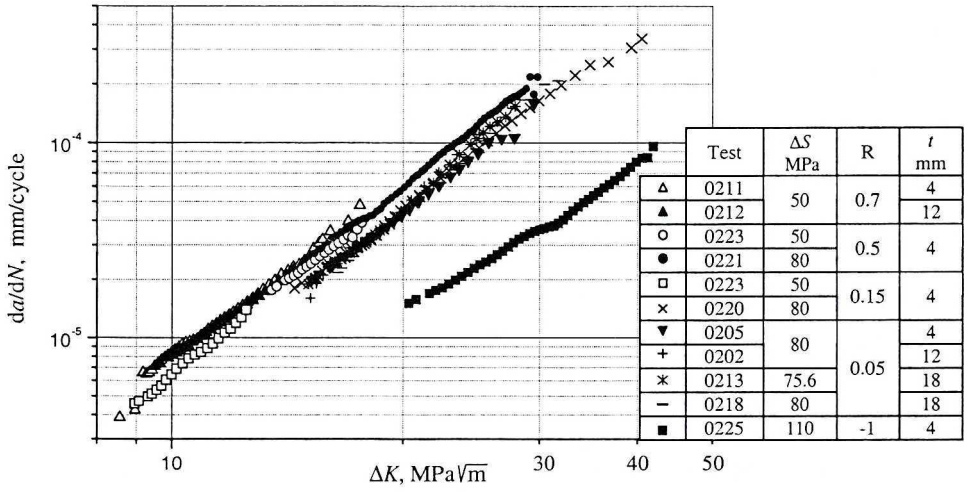

Fig. 4. Fatigue crack growth data for the CA tests

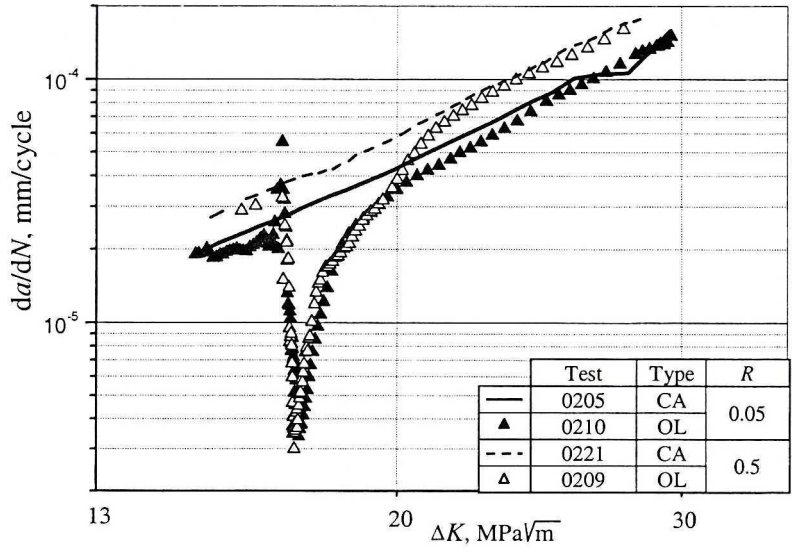

Fig. 5. Exemplary results on overload-induced delayed retardation in crack growth

The da/dN vs. ΔK results for the CA tests are plotted in Fig. 4. These data illustrate that, in agreement with the literature evidence for structural steel (e.g. [13]), no systematic influence of specimen thickness on da/dN is observed, whilst for a given specimen thickness the crack growth rates systematically increase with the R-ratio. The latter tendency is, however, insignificant as the data points from all tests performed at positive R-ratios fall into a narrow scatter band quantified by a high correlation coefficient r^2 of

0.979. Fig. 5, where the post-OL transient crack growth rates for two tests are shown, indicates that under variable amplitude loading significant load interaction effects can occur in 18G2A. Note in Fig. 4 that within the da/dN range common for the $R = 0.5$ and $R = 0.7$ tests the crack growth rates observed at $R = 0.7$ are slightly above those measured in the $R = 0.5$ tests which indicates that CC must be active at the latter R-ratio.

2.2. Crack closure measurements

All crack growth tests except those carried out at $R = 0.7$ were coupled with CC measurements using the compliance technique. Fife three-channel transducer conditioners incorporated in the fatigue machine controller were used to acquire the compliance data at a sampling rate of maximum 2 kHz per channel. The conditioners enabled the electric signal gain of 135× – 2666× and allowed smoothing the signal using a 2nd order analogue Butterworth filter with a cut-off frequency of 200 or 600 Hz. The electric signals from the load cell and the strain gauges were phase matched and converted into digital signals of a 19 bit resolution.

Table 3.

Examples of the strain gauge positions and dimensions for Method I and II

Test No.	Strain gauge positioning	Strain gauge coordinates, mm			Gauge length, mm
		Gauge	x_g	y_g	
0202	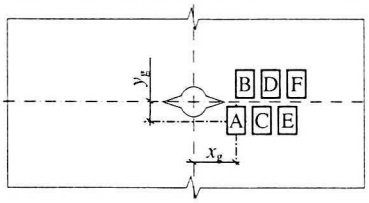	A	9	1	0.6
		B	12	1	0.6
		C	14.5	1	0.6
		D	18	1	0.6
		E	21	1	0.6
		F	23	1	0.6
0220	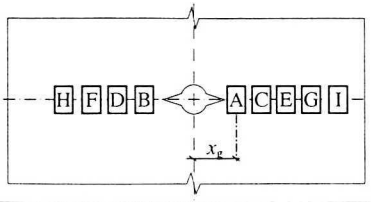	A	12.4		3
		B	14.4		3
		C	16.4		4
		D	18.4		4
		E	20.4	—	4
		F	22.4		4
		G	24.4		4
		H	27.4		6
		I	29.4		6

The arrays of near-tip strain gauges either positioned at a small distance above and below the crack path or straddling the expected crack path were used for the local compliance measurements. The above two techniques will be further referred to as Method I and II respectively. Table 2 specifies the techniques applied in individual tests whilst an exemplary positioning and dimensions of gauges are presented in Table 3.

In an effort to reduce the measurement noise, the CC measurements were conducted at various combinations of the ε signal gain, the loading and sampling frequency, and signal filtering methods [4]. Though the amount of noise on the compliance data was found to depend on a combination of the data acquisition parameters and signal filtering, the results of the ASTM method remained generally unaffected, as proved by identical results on P_{op} from Tests 0222 and 0223. In these experiments performed under the same loading conditions, different combinations of the data acquisition parameters and signal filtering were applied. This implies that the ASTM procedure is insensitive to the moderate amount of noise. As proposed by Phillips [17] and recommended by the ASTM E647 standard, the mean (CO_{mean}) and the standard deviation (σ_{CO}) of the CO_i values determined according to Eq. (2) for the raw signal before crack growth occurs can represent the compliance data quality, being a measure of nonlinearity and noise respectively in the test set up. With the present measurement system, $CO_{mean} = 0.1887\%$ and $\sigma_{CO} = 0.5162\%$, which is well below the limits of 1% and 2% respectively specified by the ASTM E647 standard.

3. Closure measurement results and discussion

Presented below are the most representative results that enable to consider the effects of various aspects of the measurement technique and data processing on CC estimates.

3.1. Effect of strain gauge distance from the crack tip

Fig. 6 shows the results on the crack opening stress (S_{op}) for Test 0202 estimated using the ASTM procedure with an offset criterion of 1%. The local compliance data come from Method I, the gage positioning being shown at the top of the figure. It is seen that the S_{op} estimates corresponding to a given strain gauge drop rapidly as the crack tip passes the gauge and then increase again. When the gauge recedes from the crack tip with further crack growth the S_{op} values gradually decrease. Results from gauge C demonstrate that for a gauge still ahead of the crack tip, the S_{op} level is gradually increasing as the crack tip approaches the gauge. Further analyses of the Method I local compliance data indicate that the effect of gauge distance from the crack tip becomes less pronounced when the offset criterion is increased and when the ASTM procedure is applied instead of the ASTM procedure.

From local compliance measurements according to Method I, Dougherty [11] reported an S_{op} behaviour qualitatively similar to that in Fig. 6. Again in

to that agreement with Dougherty's study, and also with fracture mechanics based analysis results by Pippan [18], is the observed transition in the compliance curve shape shown in Fig. 7. Interestingly, positions of the peak S_{op} values ahead and behind the crack tip in Fig. 6 conform to positions of the extreme measurement sensitivity deduced theoretically by Pippan. According to Pippan, the measurement sensitivity drops to zero when the gauge becomes very close to the crack tip, in correspondence to the dip in the S_{op} values revealed in Fig. 6 for each gauge passing the crack tip. The similarities between the results by Pippan and those in Fig. 6 suggest that with Method I, the measurement sensitivity can be quantified by the S_{op} value.

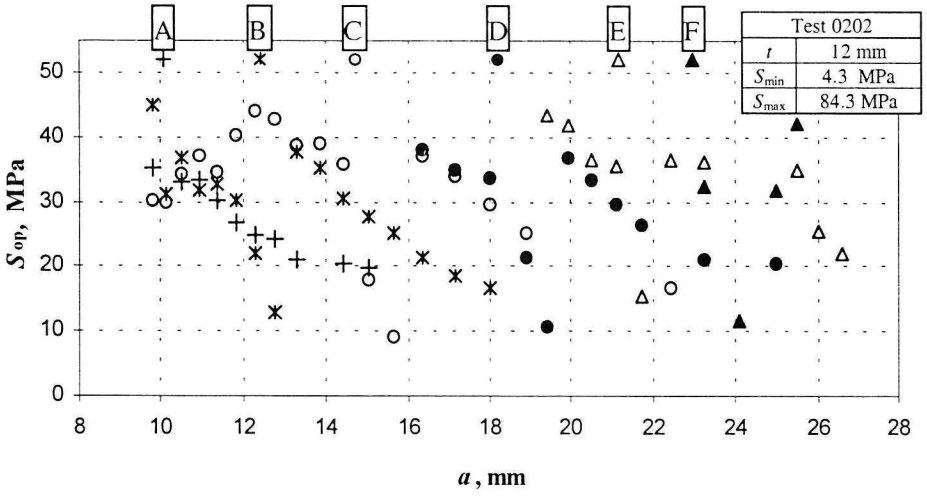

Fig. 6. Effect of the gauge position relative to the crack tip on S_{op} estimates from the Method I compliance measurements and the ASTM procedure with 1% offset criterion

The data from Test 0220 shown in Fig. 8 exemplify a dependence of the S_{op} estimates according to three different offset criteria on gauge distance from the crack tip when the local compliance records are acquired using Method II. It is evident in Fig. 8 that in that case the S_{op} value can no longer be considered a measure of the measurement sensitivity. Whether the S_{op} values from a gauge still distant from the crack tip are higher or lower than the stabilized S_{op} level corresponding to the same gauge located closer to the crack tip depends on the assumed offset criterion. The above dependence is purely an effect of measurement noise, being most pronounced in the beginning of the test when the noise-to-signal ratio can be significant due to still low local cyclic strains. As these strains are increasing with crack growth, the noise-to-signal ratio is decreasing, which yields a diminishing sensitivity of the S_{op} estimates to gauge distance shown in Fig. 8 by the results obtained for all offset criteria.

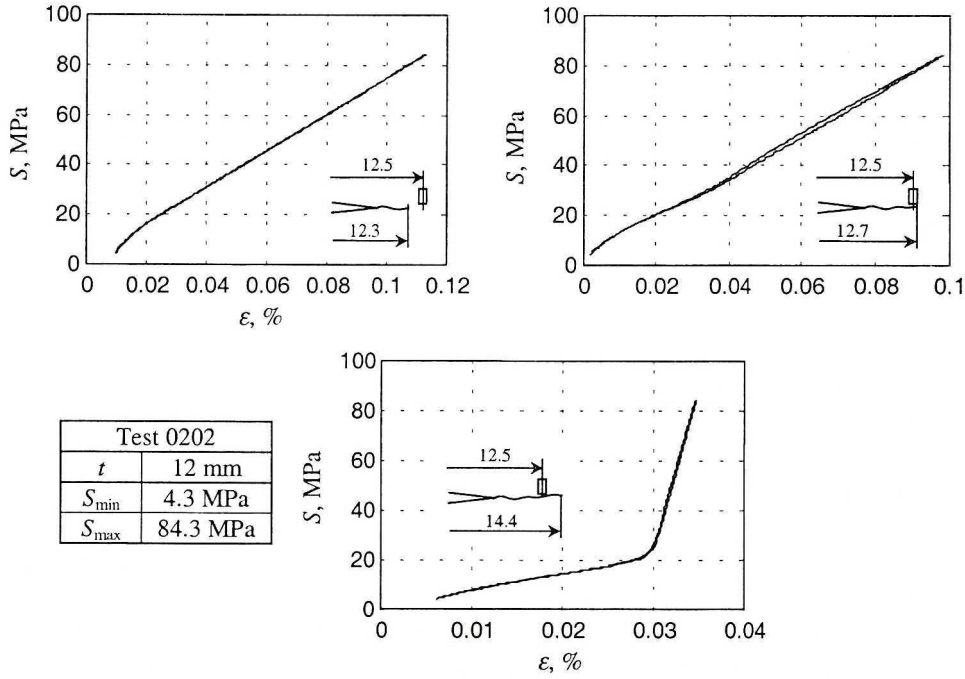

Fig. 7. Effect of the gauge position relative to the crack tip on the compliance curve shape from the Method I local compliance measurements

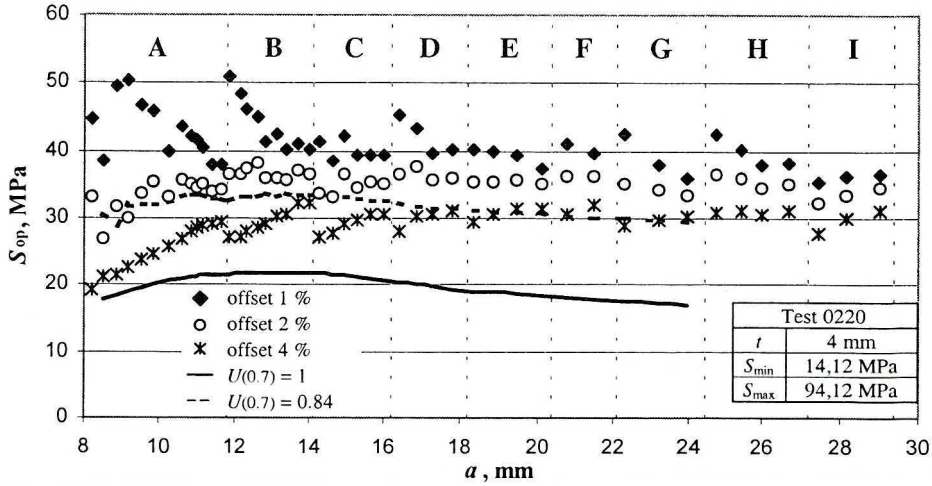

Fig. 8. Effect of gauge distance from the crack tip on S_{op} estimates from the Method II compliance measurements and the ASTM procedure for various offset criteria

Results of other tests confirm the trend already evident from Figs 6 and 8, namely that in comparison with Method I, Method II enables to obtain stabilized S_{op} values over a much longer crack growth interval and yields less scatter. A dependence of the S_{op} estimates on the gauge position exhibited, though in various degrees, by either technique is a premise to further consider only local compliance records acquired from a gauge closest to the crack tip (for Method I ahead of the crack tip).

3.2. Choice of the offset criterion

The results considered in the previous section reveal that Method II is more robust that Method I. Hence, an offset criterion appropriate for structural steel will be selected based on the results from Method II.

As already shown in Fig. 8, the S_{op} estimates from the ASTM procedure strongly depend on the assumed value of the offset criterion. In order to select an offset appropriate for structural steel, the results of Test 0211 and 0212 conducted at an R-ratio of 0.7 are employed. Donald and Paris [19] reported that for Al alloys, processing the compliance data using the ASTM method revealed no evidence of non-linearity in the P-ε plots at so high an R-ratio. Consequently, they considered the $R = 0.7$ data closure-free and used them as the basis for evaluating various methods of estimating ΔK_{eff}. However, finite element results of Tsukuda et al. [16] did indicate the occurrence of plasticity-induced CC in structural steel at $R = 0.7$. Their analyses showed the distance behind the crack tip over which the crack was closed at minimum load to decrease from 0.4 mm at $R = 0$ to 0.016 mm at $R = 0.7$. On the other hand, at $R \geq 0.5$ Tsukuda et al. [16] detected no closure for specimens of structural steel in local compliance measurements employing Method I, according to the present study terminology. Altogether, the results from Refs [16], [19] suggest that compliance changes associated with the CC phenomenon at high R-ratios can be too small to be reflected in the P-ε diagrams. Notably, an equation proposed by Schijve [20] to estimate CC levels in 2024 Al-alloy and shown recently to provide a satisfactory correlation of the R-ratio effect also for D16 Al-alloy [21], yields an U ($=\Delta K_{eff}/\Delta K$) value of 0.84 for $R = 0.7$. The same U value for $R = 0.7$ follows, otherwise, from the aforementioned finite element analyses [16].

Given the uncertainties about the occurrence of CC at $R = 0.7$, it is assumed here that acceptable S_{op} estimates should fall within the bounds corresponding to $U = 0.84$ and $U = 1$ for the $R = 0.7$ tests (0211 and 0212, Table 2). The bounding S_{op} levels for each $R < 0.7$ test were computed under the assumption that within the da/dN range common for that test and for the

$R = 0.7$ tests the same crack growth rates imply the same ΔK_{eff} values at both R-ratios. Because the average value of the Paris law exponent for the CA data in Fig. 4 equals 3.28, the above-defined bounds of acceptable S_{op} estimates yield a factor of 1.8 ($=0.84^{-3.28}$) difference in the da/dN values corresponding to the upper and lower S_{op} limit.

Figs 8 and 9 show the effect of the offset criterion assumed in the ASTM procedure on the S_{op} results from the Method II local compliance measurements performed at four R-ratio values. Plotted for each test are the lower and upper bound of the acceptable results denoted as $U(0.7) = 1$ and $U(0.7) = 0.84$. Unlike the offset criteria of 1% and 2%, the 4% criterion indicates $S_{op} = S_{min}$ at $R = 0.5$ (Fig. 9c) and it is not capable to detect the CC transients after the 1st OL applied in the 2OL test (Fig. 9b). Fig. 9c demonstrates that for the R=0.15 part of Test 0223, the results from all offset criteria fall within the acceptable range. However, for Test 0220 performed at the same R-ratio but at a higher applied stress range (ΔS) only the stationary 4% offset results merge with the upper S_{op} bound, Fig. 8. Figs 8 and 9 further indicate that the influence of the offset criterion on S_{op} is marked at $R = 0.07$ and $R = 0.15$ and much weaker at $R = 0.5$ and $R = -1$. A closer examination of the compliance data has revealed that the latter behaviour is associated with the dependence of the *P-CO* diagram shape on the R-ratio. The $R = 0.15$ *P-CO* curves are steep in the near-S_{op} region, which results in a high sensitivity of the S_{op} values to the offset criterion level, whilst the low sensitivity at $R = 0.5$ and $R = -1$ stems from the flatness of the corresponding *P-CO* curves.

A general conclusion from Figs 8 and 9 is that of the offset criteria considered only the 4% value produces for all CA tests the S_{op} estimates falling still within or very close to the acceptable range. Hence, the 4% offset has been selected for further applications of the ASTM procedure.

With the nASTM procedure, it has been found that the mean S_{op} stresses produced for the normalized compliance offset (CO/CO_{max}) criteria of 8, 12 and 20% give a best overall correlation with the S_{op} results obtained for 1, 2 and 4% criteria respectively using the ASTM procedure. Consequently, the criterion of 20% has been selected to compare the nASTM procedure with the ASTM procedure associated with the 4% criterion. Examples of S_{op} estimates obtained at the 20% criterion from the nASTM method set against those produced by the ASTM method with the 4% criterion are given in Fig. 10.

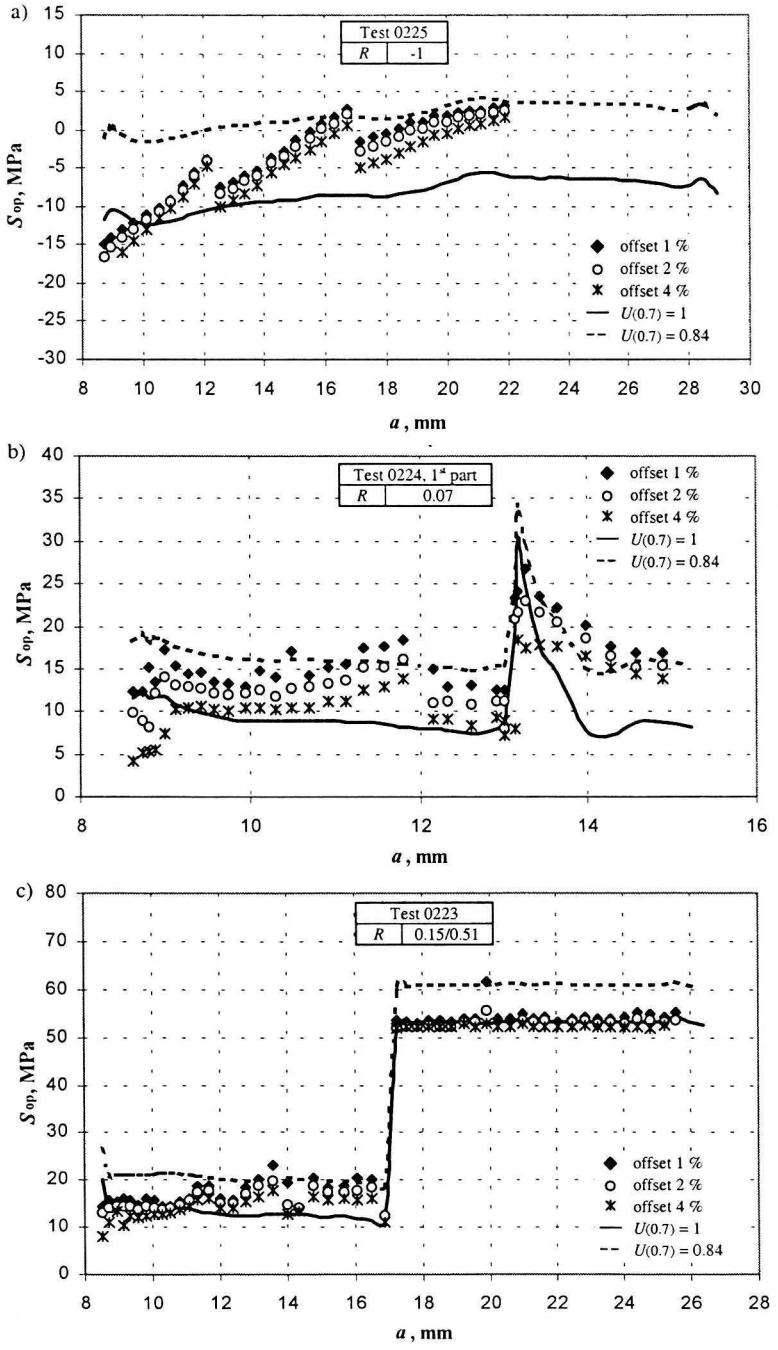

Fig. 9. Influence of the compliance offset criterion value on S_{op} estimates from the Method II compliance measurements and the ASTM procedure: (a) $R = -1$; (b) $R = 0.07$; (c) $R = 0.15$ and 0.51

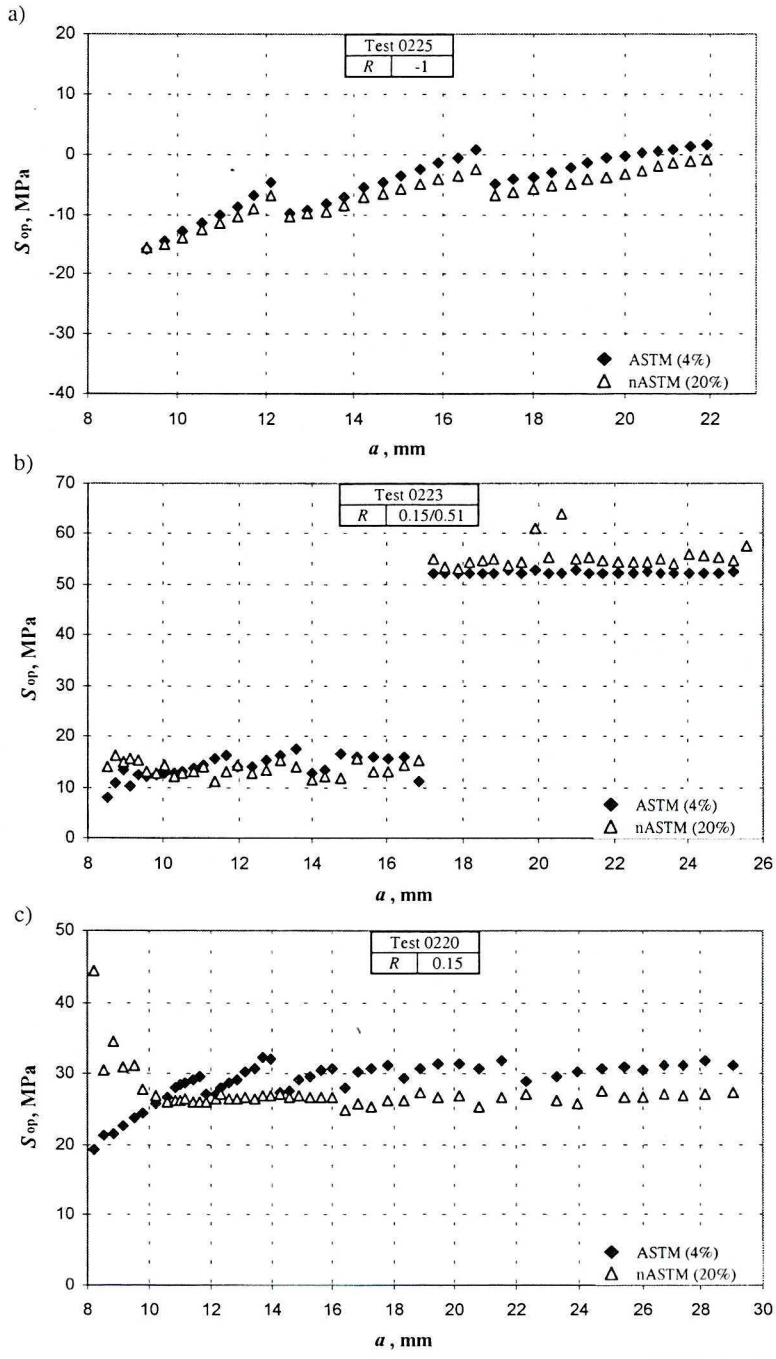

Fig. 10. Comparisons between S_{op} estimates from the Method II compliance records produced by the ASTM procedure at the 4% offset criterion and by the nASTM procedure at the 20% offset criterion: (a) $R = -1$; (b) $R = 0.15$ ($\Delta S = 50.4$ MPa) and 0.5; (c) $R = 0.15$ ($\Delta S = 80$ MPa)

4. Correlation with fatigue crack growth rates

Figs 11a and b give the da/dN vs. ΔK_{eff} data based on the S_{op} values obtained via processing the Method I compliance records using the ASTM and nASTM procedure respectively. Also plotted the full line and dashed line respectively are the da/dN vs. ΔK and da/dN vs. $(0.84\Delta K)$ regression lines for the $R = 0.7$ test data.

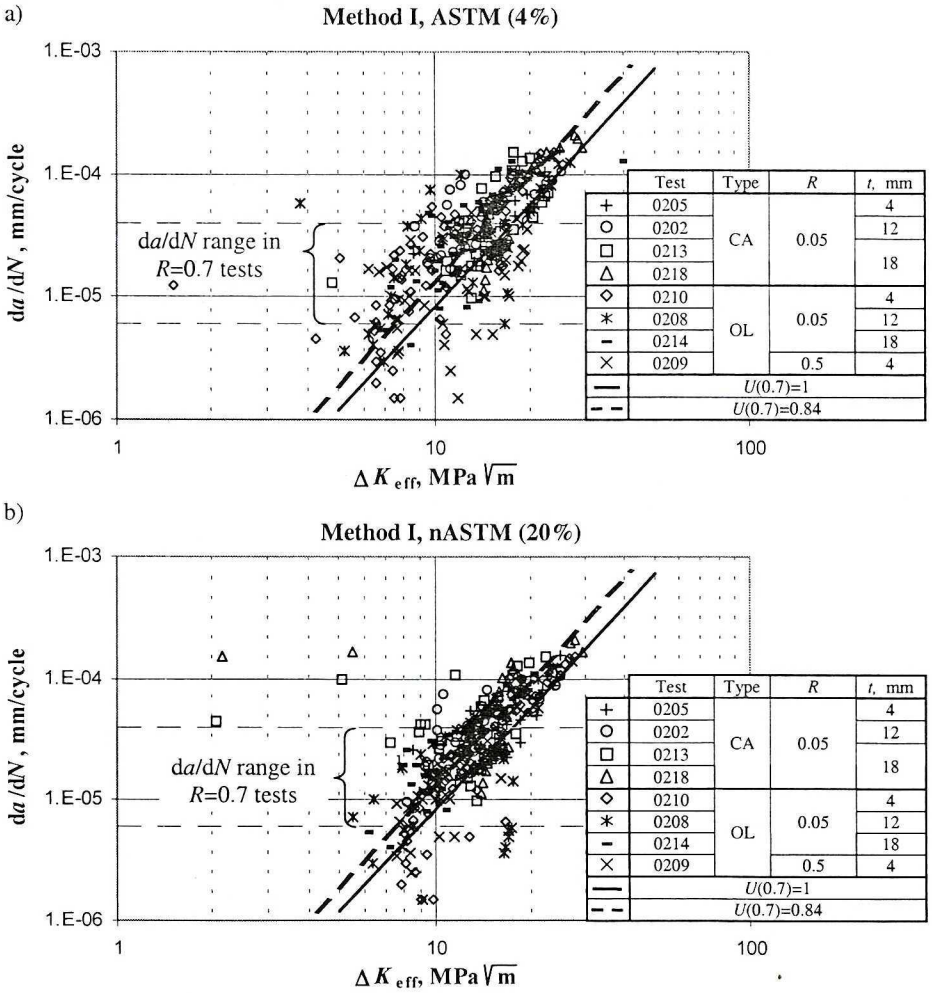

Fig. 11. da/dN vs. ΔK_{eff} data based on the S_{op} values from the Method I compliance records and: (a) the ASTM procedure; (b) nASTM procedure

A dramatic scatter shown by the results in Fig. 11 could be anticipated from the unstable nature of the S_{op} values corresponding to the Method I measurement technique (compare Fig. 6). However, compared to the ASTM procedure, the nASTM procedure yields a better overall consolidation of the

data, as also noted in the aforementioned study by Song and Kang [6]. Surprisingly enough, the nASTM procedure has the power of absorbing some drastically outlying data points produced by the ASTM procedure and vice versa. In view of that, the most outlying points on the very left of Figs. 11a and b come from different tests, namely from the OL tests for the ASTM procedure and CA tests for the nASTM procedure.

In Figs 12a and b, to those in Fig. 11 results obtained from the Method II compliance measurements are shown. It is evident that the ΔK_{eff} parameter reconciles the crack growth rates observed under various loading conditions incomparably better than in Fig. 11. Again, the nASTM procedure produces slightly less scatter than the ASTM procedure, as quantified by the correlation coefficient of 0.985 and 0.968 respectively. The r^2 values have been computed after rejecting the drastically outlying data points according to Student's test assuming a 0.99 probability level [22]. However, all the data points are preserved in Figs. 12a and b to demonstrate that all the outliers seen on the far left in Fig. 12a have been absorbed when applying the nASTM procedure. For Test 0224, the effect of the 1st OL is not correlated, as one could expect considering Fig. 9b. However, the data points corresponding to the retarded crack growth following the 2nd OL do fall within the acceptable range, i.e. between the $U(0.7) = 1$ and $U(0.7) = 0.84$ lines. A further confirmation that the crack growth transients induced by the 2nd OL are correctly accounted for comes from Fig. 13 where the crack growth rates observed and predicted based on the CC measurements are compared. Here, the predicted rates have been computed using the master $da/dN = C(\Delta K_{\text{eff}})^m$ relationship fitting the CA data from Fig. 12b with the ΔK_{eff} values determined for the S_{op} levels according to the nASTM procedure and the Method II measurement technique. For the 2nd part of the 2OL test, the conformance of both type results is satisfactory. Note a good agreement in the recovery stage from the minimum crack growth rates where most researchers report the results inferred from CC to be lower than the observed data (e.g. [23]).

The quality of the Method II results, Fig. 12, is more satisfactory than in the case of some works cited above, otherwise employing the Method I technique found in the present study to be inferior to Method II. However, the present work has revealed unquestionable drawbacks of the ASTM method even if coupled with Method II, like an insufficient sensitivity at low strain levels and/or high R-ratio values and – for a given offset criterion – oscillations of S_{op} between the lower and higher limiting level depending on the loading conditions. A closer examination of the P-CO plots indicates that at positive R-ratios the CO parameter adopts a negative initial value at $P_{\max}$ and gradually tends towards zero within the "open crack" portion of a load

cycle. Because the above behaviour arises from the hysteresis and curvature of the local P-ε data, it becomes more pronounced with increasing the R-value and the applied stress range, as exemplified in Fig. 14. In general, the compliance data produced in the present study provide a large body of evidence to prove that the "open crack" compliance cannot be considered constant and thus imply that the assumption of a constant compliance for the fully open crack is obviously less adequate for structural steel than for non-ferrous alloys. In view of that, worth considering are non-conventional approaches to identify P_{op} which, like an algorithm proposed by the present authors [4], [24], do account for the open crack compliance variations.

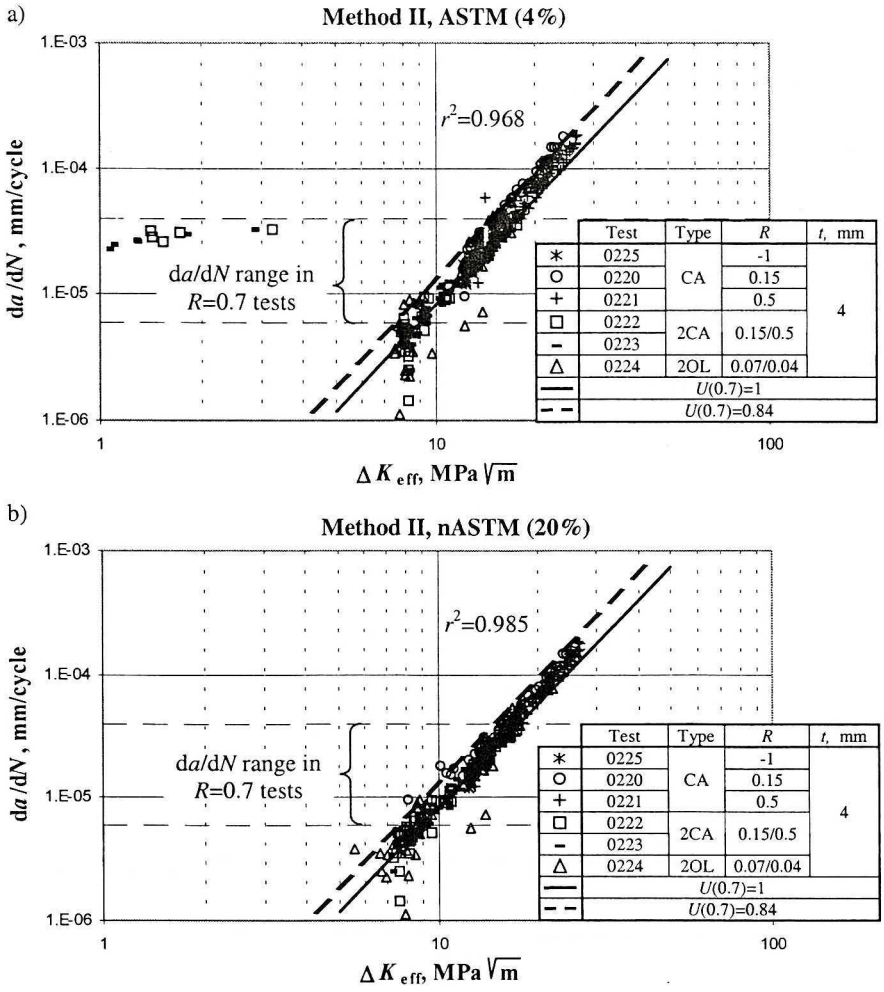

Fig. 12. da/dN vs. ΔK_{eff} data based on the S_{op} values from the Method II compliance records and: (a) the ASTM procedure; (b) nASTM procedure

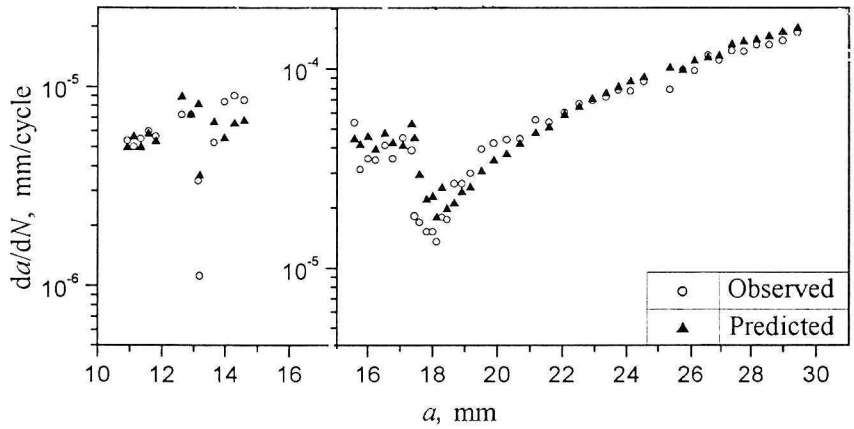

Fig. 13. Comparisons between the crack growth rates observed and inferred from the CC measurements for Test 0224 (Method II, nASTM 20%)

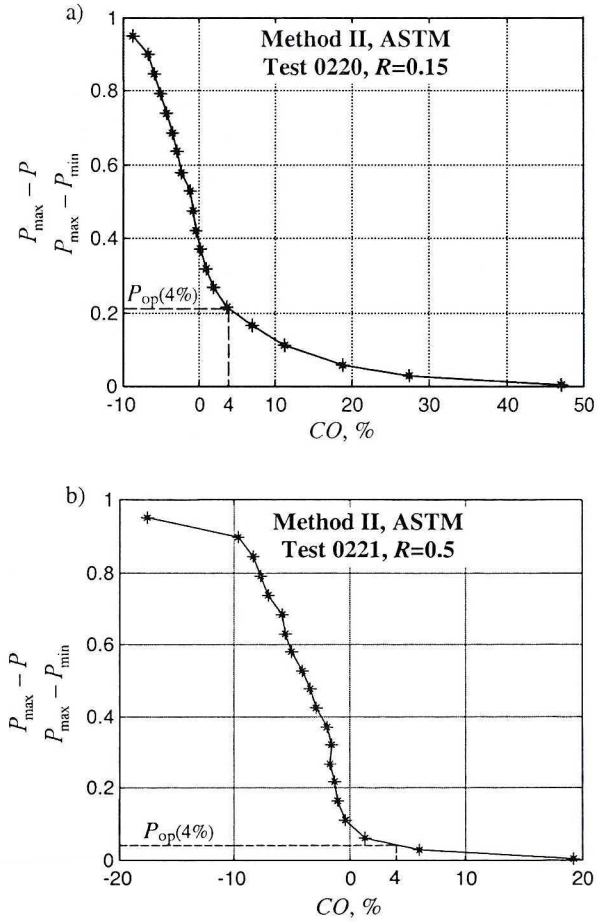

Fig. 14. Examples of Load-Compliance Offset diagrams from the Method II CC measurements: (a) Test 0220; (b) Test 0221

5. Conclusions

1. Some crack closure (CC) measurement techniques using the elastic compliance method and procedures for the identification of the crack opening load (P_{op}) from compliance data suitable for non-ferrous alloys may not be such for structural steel because of their insufficient sensitivity and differences in the shape of the compliance traces for both groups of metals. Specifically, the remote compliance technique typically applied for Al alloys and curve-fitting procedures reported to be most appropriate for Al alloys are inadequate for structural steel.

2. Out of the conventional procedures for CC estimates, i.e. those assuming a constant compliance value for the fully open crack, applicable to structural steel, the ASTM method is least subjective in identifying the CC level and insensitive to small amounts of measurement noise.

3. CC measurement results from local strain gauges positioned ahead of the crack tip across the expected crack path (Method II) are considerably more consistent than those from local gauges mounted at a small distance above the crack path (Method I), otherwise more often used. In view of that, the crack growth rate (da/dN) vs. effective stress intensity factor range (ΔK_{eff}) data based on the Method I compliance measurements show incomparably more scatter than the same type data corresponding to Method II.

4. Only the 4% offset criterion for the ASTM procedure and the 20% offset criterion for the normalized ASTM (nASTM) procedure provided CC estimates falling within or very close to a preset range of acceptable data, which has been defined based on results of the constant amplitude tests conducted at a stress ratio of 0.7. However, when coupled with so a high offset value, either procedure shows an insufficient sensitivity at low strain levels and at a high load ratio. The sensitivity of the results on P_{op} to the assumed offset value depends on the loading conditions.

5. A consolidation of the crack growth rates measured under a variety of loading conditions presented against the ΔK_{eff} parameter based on the Method II CC measurements is generally better than reported in the literature. In terms of scatter of the da/dN vs. ΔK_{eff} data the nASTM procedure always yields results superior to the original ASTM procedure.

6. A closer examination of the compliance data generated in the present experiments reveals that compliance is typically variable over the whole load range, against the basic assumption adopted in the ASTM procedure and most methods for evaluating CC. The latter observation suggests a need of considering applicability of non-conventional approaches which do account for the open crack compliance variations.

The authors would like to acknowledge a partial financial support from the KBN project No. 4 T07C 018 26.

Manuscript received by Editorial Board, February 27, 2004;
final version, May 11, 2004.

REFERENCES

[1] Elber W.: Fatigue crack closure under cyclic tension. Engng Fracture Mech., 1970, Vol. 2, pp. 37÷45.

[2] Skorupa M.: Load interaction effects during fatigue crack growth under variable amplitude loading – a literature review. Part II: qualitative interpretation. Fatigue Fract. Engng Mater. Struct., 1999, Vol. 22, pp. 905÷926.

[3] Skorupa M.: Experimental investigation of fatigue crack closure. In: Experimental Methods in Fatigue of Materials and Structures. A Collection of Monographs. Edited by J. Szala. Wydawnictwa Uczelniane Akademii Techniczno-Rolniczej, Bydgoszcz. 2000, pp. 149÷206 (*in Polish*).

[4] Machniewicz T.: Experimental analysis of fatigue crack closure for structural steel. Ph.D. Thesis. AGH University of Science and Technology, Kraków, 2003 (*in Polish*).

[5] ASTM Standard E 647-95. Standard test method for measurement of fatigue crack growth rates. ASTM Annual Book of ASTM Standards, Philadelphia, 1995.

[6] Song J. H., Kang J. Y.: Quantitative evaluation of K_{op} determination and ΔK_{eff} estimation methods. Fatigue 2002, Proceedings of the Eighth International Fatigue Congress held 3-7 June 2002, Edited by Blom A.F., Stockholm 2002, Vol. 4, pp. 2345÷2352.

[7] Carman C. D., Turner C. C., Hilberry B. M.: A method for determining crack opening load from load-displacement data. ASTM STP 982, 1988, pp. 214÷221.

[8] Yisheng W., Schijve J.: Fatigue crack closure measurements on 2024-T3 sheet specimens. Fatigue Fract. Engng Mater. Struct., 1995, Vol. 18, pp. 917÷921.

[9] Xu Y., Gregson P. J., Sinclair I.: Systematic assessment and validation of compliance-based crack closure measurements in fatigue. Materials Science and Engineering, 2000, A284, pp. 114÷125.

[10] Kikukawa M., Jono M., Tanaka K.: Fatigue crack closure behaviour at low stress intensity factor level. Proc. 2nd Int. Conf. Mechanical Behaviour of Materials (ICM-2), 1976, Special Vol., pp. 254÷277.

[11] Dougherty J. D.: Combined experimental and finite element study of fatigue crack closure in 1070M steel. Ph.D. Thesis, The University of Akron, OH, USA, 1994.

[12] Tokaji K., Ando Z., Nagae K., Imai T.: Effect of sheet thickness on fatigue crack retardation and validity of crack closure concept. Proc. 2nd Int. Conf. Fatigue and Fatigue Thresholds. Univ. of Birmingham, 1984, Vol. II, pp. 727÷737.

[13] Fleck N. A.: An investigation of fatigue crack closure. Cambridge University Engineering Dept. report CUED/C-MATS/TR.104, May 1984.

[14] Kurihara M., Katoh A., Kawahara M.: Effects of stress ratio and step loading on fatigue crack propagation rate. Current Research on Fatigue Cracks. Materials Research Series. The Society of Materials Science, Japan 1985, Vol. 1, pp. 217÷233.

[15] Ohta A., Kosuge M., Sasaki E.: Fatigue crack closure over the range of stress ratios from – 1 to 0.8 down to stress intensity threshold level in HT80 steel and SUS304 stainless steel. Int. J. Fracture, 1978, Vol. 14, pp. 251÷264.

[16] Tsukuda H., Ogiyama H., Shiraishi T.: Fatigue crack growth and closure at high stress ratios. Fatigue Fract. Engng Mater. Struct., 1995, Vol. 18, pp. 503÷514.
[17] Phillips E. P.: Results of the second round robin on opening-load measurement conducted by ASTM task group E24.04.04 on crack closure measurement and analysis. NASA Techn. Memorandum 109032, NASA, Langley Research Center, Hampton, Virginia 23681-0001, 1993.
[18] Pippan R.: The sensitivity to measure crack closure with strain gauges near the crack tip. Engng Fracture Mech., 1988, Vol. 31, pp. 867÷871.
[19] Donald J. K., Paris P. C.: An evaluation of ΔK_{eff} estimation procedures on 6061-T6 and 2024-T3 aluminium alloys. Int. J. Fatigue, 1999, Vol. 21, pp. S47÷S57.
[20] Schijve J.: Some formulas for the crack opening stress level, Engng Fracture Mech, 1981, Vol. 14, pp. 461÷465.
[21] Schijve J., Skorupa M., Skorupa A., Machniewicz T., Gruszczyński P.: Fatigue crack growth in the aluminium alloy D16 under constant and variable amplitude loading. Int. J. Fatigue, 2004, Vol. 26, pp. 1÷15.
[22] Rokosz A.: Statistical Methods, PWT Warszawa, 1957 (*in Polish*).
[23] Fleck N. A.: Influence of stress state on crack growth retardation. ASTM STP 924, 1988, Vol. 1, pp. 157÷183.
[24] Skorupa M., Beretta S., Carboni M., Machniewicz T.: An algorithm for evaluating crack closure from local compliance measurements. Fatigue Fract. Engng Mater. Struct., 2000, Vol. 25, pp. 261÷273.

Wyznaczanie poziomu zamykania się pęknięcia w stali konstrukcyjnej na podstawie lokalnych pomiarów podatności

Streszczenie

W artykule rozważono możliwość oszacowania poziomu zamykania się pęknięcia w stali konstrukcyjnej na podstawie pomiaru podatności sprężystej z wykorzystaniem procedur opartych na konwencjonalnym założeniu, że podatność próbki z otwartym w pełni pęknięciem jest stała. Spośród możliwych do zastosowania technik pomiarowych i koncepcji wyznaczania poziomu otwarcia pęknięcia za najodpowiedniejszą uznano metodą zalecaną przez normę ASTM, której przydatność w zastosowaniu do stali konstrukcyjnej nie została dotąd sprawdzona. Dane podatności, zarejestrowane w trakcie badań zmęczeniowych stali 18G2A, prowadzonych przy różnych typach obciążenia, pozwoliły na zbadanie wpływu techniki pomiarowej i wartości przyjmowanych w metodzie ASTM kryteriów na oceny zamykania się pęknięcia. Adekwatność zastosowanych opcji pomiarowych i procedur obliczeniowych zbadano rozważając korelacje pomiędzy wynikami pomiarów zamykania się pęknięcia i zaobserwowanymi prędkościami wzrostu pęknięć.